



HAL
open science

Expected temporal Absolute Gravity change across the Taiwanese Orogen, a modeling approach

M. Mouyen, F. Masson, C. Hwang, C.-C. Cheng, R. Cattin, C.W. Lee, Nicolas Lemoigne, J. Hinderer, Jacques Malavieille, R. Bayer, et al.

► **To cite this version:**

M. Mouyen, F. Masson, C. Hwang, C.-C. Cheng, R. Cattin, et al.. Expected temporal Absolute Gravity change across the Taiwanese Orogen, a modeling approach. *Journal of Geodynamics*, 2009, 48 (3-5), pp.284. 10.1016/j.jog.2009.09.004 . hal-00594426

HAL Id: hal-00594426

<https://hal.science/hal-00594426v1>

Submitted on 20 May 2011

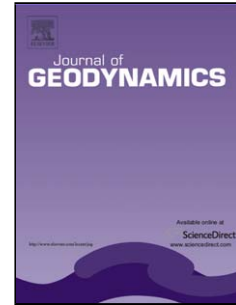
HAL is a multi-disciplinary open access archive for the deposit and dissemination of scientific research documents, whether they are published or not. The documents may come from teaching and research institutions in France or abroad, or from public or private research centers.

L'archive ouverte pluridisciplinaire **HAL**, est destinée au dépôt et à la diffusion de documents scientifiques de niveau recherche, publiés ou non, émanant des établissements d'enseignement et de recherche français ou étrangers, des laboratoires publics ou privés.

Accepted Manuscript

Title: Expected temporal Absolute Gravity change across the Taiwanese Orogen, a modeling approach

Authors: M. Mouyen, F. Masson, C. Hwang, C.-C. Cheng, R. Cattin, C.W. Lee, N. Le Moigne, J. Hinderer, J. Malavieille, R. Bayer, B. Luck



PII: S0264-3707(09)00071-4
DOI: doi:10.1016/j.jog.2009.09.004
Reference: GEOD 898

To appear in: *Journal of Geodynamics*

Please cite this article as: Mouyen, M., Masson, F., Hwang, C., Cheng, C.-C., Cattin, R., Lee, C.W., Le Moigne, N., Hinderer, J., Malavieille, J., Bayer, R., Luck, B., Expected temporal Absolute Gravity change across the Taiwanese Orogen, a modeling approach, *Journal of Geodynamics* (2008), doi:10.1016/j.jog.2009.09.004

This is a PDF file of an unedited manuscript that has been accepted for publication. As a service to our customers we are providing this early version of the manuscript. The manuscript will undergo copyediting, typesetting, and review of the resulting proof before it is published in its final form. Please note that during the production process errors may be discovered which could affect the content, and all legal disclaimers that apply to the journal pertain.

Expected temporal Absolute Gravity change across the Taiwanese Orogen, a modeling approach

M. Mouyen^{*,a}, F. Masson^a, C. Hwang^b, C.-C. Cheng^b, R. Cattin^c, C.W. Lee^d, N. Le Moigne^c, J. Hinderer^a, J. Malavieille^c, R. Bayer^c, B. Luck^a

^a*Institut de Physique du Globe de Strasbourg, 5 rue René Descartes, F-67084 Strasbourg cedex, France*

^b*Department of Civil Engineering, National Chiao Tung University, 1001 University Road, Hsinchu, Taiwan 300, R.O.C.*

^c*Géosciences Montpellier, Université Montpellier 2, Place E. Bataillon, 34095 Montpellier cedex 5, France*

^d*Center for Measurement Standards, Industrial Technology Research Institute, 195 Chung Hsing Rd., Sec.4 Chu Tung, HsinChu, Taiwan 310, R.O.C.*

Abstract

The island of Taiwan is located on the convergent boundary between the Philippine Sea plate and the Chinese continental margin. It offers very active mountain building and collapsing processes well illustrated by the rugged topography, rapid uplift and denudation, young tectonic landforms, active faulting and numerous earthquakes. In this paper, using simple models, we have estimated vertical movements and associated absolute gravity variations which can be expected along a profile crossing the southern part of the island and probably suffering the highest rates of rising. The two different tectonic styles proposed for the island, thin-skinned and thick-skinned, were taken into account. Horizontal and vertical movements were modeled by an elastic deformation code. Gravity variations due to these deformations are

*Corresponding author. Tel.: +33 3 90 24 00 77; fax: +33 3 90 24 02 91.

Email address: maxime.mouyen@eost.u-strasbg.fr (M. Mouyen)

then modeled at a second step. They are dominated by plate and free air effects, i.e. elevation of the topography, with several $\mu\text{Gal yr}^{-1}$. By comparison, gravity changes generated by mass transfers are weak: maximum $0.1 \mu\text{Gal yr}^{-1}$ with the thin-skinned tectonic and $0.3 \mu\text{Gal yr}^{-1}$ with the thick-skinned tectonic. Though elastic rheology has limitations, this modeling offers interesting results on what gravity signal can be expected from the AGTO project (Absolute Gravity in the Taiwanese Orogen), which proposes to study the dynamic of these mountain ranges using absolute gravimetry (AG) and also including relative gravimetry (RG) and GPS measurements.

Key words: Taiwan, Gravity, Modeling, Surrection, Mass transfers

1. Introduction

Global Positioning System (GPS) and absolute gravimetry are useful tools to study vertical movements and mass transfers involved in mountain building (Segall & Davis, 1997; Torge, 1990). Combining both tools improves understanding of tectonic processes. As an application Karner & Watts (1983) showed how the variation of the ratio between gravity rate and elevation rate across a mountain range can be related to the elastic thickness of the crust. The AGTO project proposes to study the Taiwan orogeny using absolute and relative gravity measurements, GPS and modeling, in order to jointly identify vertical movements and mass transfer. Taiwan, experiencing vigorous mountain building processes, is a convergence zone located West of south China, between the Chinese Sea and the Philippine Sea (figure 1 a). The AGTO project is part of two issues. First is to validate the use of absolute gravity for tectonic purposes. Second is to improve our understanding of the

15 Taiwanese orogeny providing information on vertical movements and mass
16 transfers.

17 **Insert figure 1**

18 The AGTO project focuses on the south part of Taiwan, along a East-West
19 transect crossing the whole island (figure 1 b). Nine sites have been defined
20 for absolute gravity measurements, close to permanent GPS stations from the
21 Taiwan GPS network. A concrete pillar has been built at each site to put
22 the FG5 absolute gravimeter. In addition a wider network of 53 sites around
23 this transect has been defined for relative gravity measurements (figure 1).
24 It is divided into 9 loops, each containing at least one AG site. This relative
25 gravity network has also been carefully mapped on the Taiwan GPS network,
26 for precise correlation between the gravity signal and the elevation rate. The
27 absolute gravity measurement are repeated every year, using French and Tai-
28 wanese FG5 gravimeters. Scintrex CG5 gravimeters are used for the relative
29 network.

30 The AGTO project is still at its beginning and no conclusion is available
31 yet. In this article, using a modeling approach, we try to characterize grav-
32 ity variations expected. We start from a 2D structural section of Taiwan
33 and we model the elastic deformation that we constrain with horizontal GPS
34 velocities. Once the modeled horizontal movements fit the measured ones,
35 densities are assigned to Taiwan regions, depending on their geology. Com-
36 bining deformations and densities, a change in the gravity signal is finally
37 modeled. Two programs have been used to perform this modeling: one for
38 the elastic deformation and one for the gravity change.

39 After making a global overview of the tectonic context in Taiwan region, we

40 will describe the results we obtained from the elastic modeling and its gravity
41 implication.

42 **2. Tectonic settings**

43 Taiwan island is at the junction of the Philippine Sea plate and the
44 Eurasian plate (figure 1 a) and results from the convergence of the Luzon
45 volcanic arc on the Philippine Sea plate toward the Chinese continental mar-
46 gin on the Eurasian plate. In the North-East, the Philippine Sea plate is
47 subducted beneath the Eurasian plate. This is expressed by the Ryukyu
48 Trench in the sea ground. More to the South, the situation is the opposite;
49 the Eurasian plate is subducted by the Philippine Sea plate, generating the
50 Manila Trench (Angelier, 1986). In Taiwan, the plate boundary is underlined
51 by the Longitudinal Valley separating the Eurasian plate to the West and
52 the Philippine Sea plate to the East.

53 The collision between the Luzon arc and the Chinese continental margin
54 started 6.5 Myr. ago in the North of the island. Owing to oblique con-
55 vergence of these two regions, collision is progressing southward at a rate of
56 31 mm yr^{-1} (Simoes & Avouac, 2006). Today the Taiwanese orogen reach an
57 altitude of $\sim 4000 \text{ m}$ and is still growing (Ho, 1986; Simoes & Avouac, 2006).
58 Ho (1986) divided Taiwan into five geological regions (figure 1 b). From West
59 to East he identified the Coastal Plain, the Western foothills, the Slate Belt,
60 the Central Range and the Coastal Range. We keep this nomenclature in the
61 following study. The Coastal Plain is made of Neogene sediments overlapped
62 by quaternary alluvium, without relief. The apparition of topography to the
63 East indicates the beginning of the Western Foothills, a fold-and-thrust belt.

64 It extends to the East up to the Tulungwan fault. The Slate Belt is bounded
65 by this fault to the West and by the Lishan fault to the East. It is mostly
66 constituted by Eocene to Oligocene sediments. The Central Range, from the
67 East of Lishan fault to the Longitudinal Valley, is the most deformed part of
68 the Taiwan orogen. It shows Cenozoic clays with moderate metamorphism on
69 its west flank and more metamorphosed rocks from the pre-Tertiary basement
70 (Eurasian Continental crust) on its East flank. The Longitudinal Valley is
71 a narrow topographic depression limiting the Central range and the Coastal
72 Range. It contains the Longitudinal Valley fault, the suture zone between
73 the Eurasian and Philippine sea plates. At last, to the eastern part, the
74 Coastal Range, a remnant part of the Luzon volcanic arc mainly constituted
75 by Neogene andesite rocks and turbidite sediments, increases the topography.
76 Collision, orogeny and subduction processes in Taiwan are among the most
77 vigorous of the Earth and make this region tectonically very active. A first
78 explanation of such activity is the fast convergence of the Philippine Sea
79 plate toward the Eurasian plate, which has been evaluated to 82 mm yr^{-1}
80 (Yu et al., 1997). High ground movements have been measured by GPS and
81 a high seismicity rate is also recorded due to subduction and numerous ac-
82 tive faults. The 1999 Chi-Chi earthquake on the Chelungpu fault, the largest
83 event recorded in Taiwan ($M_w = 7.6$), illustrates this activity.

84 No tectonic style of the collision between the Luzon arc and the Chinese con-
85 tinental margin is unanimously accepted. Two main hypothesis are generally
86 discussed: the thin-skinned tectonic (Suppe, 1980; Davis et al., 1983; Dahlen
87 et al., 1984) and the thick-skinned tectonic (Wu et al., 1997; Hung et al.,
88 1999; Mouthereau & Petit, 2003). The geometry of the island cross-sections

89 will be different depending on the hypothesis taken into account and, con-
90 sequently, the results of the modeling too. As the aim of this study is not
91 to choose between one of these two tectonics but only to see their effects in
92 term of gravity, both will be used.

93 *2.1. Thin-skinned tectonic*

94 This hypothesis often held for the Taiwanese orogen. Chapple (1978)
95 defines thin-skinned fold-and-thrust belts parameters and considers that the
96 global mechanics of these accretionary wedges is similar to those of the prisms
97 which form in front of bulldozers. This theory has been tested by Davis et
98 al. (1983) and Dahlen et al. (1984).

99 Davis et al. (1983) develop an analytic theory, which predicts the critical
100 deformation of the prism materials in a compressive context. They quan-
101 titatively test this theory for the Taiwanese accretionary prism and obtain
102 results in agreement with field observations. They suggest that the detach-
103 ment is at the basal part of the Neogene continental margin, Dahlen et al.
104 (1984) more precisely identified it in the Miocene and Pliocene layers. To
105 define the thin-skinned cross section (figure 2), we use a model inspired from
106 the cross-section drawn by Malavieille & Trullenque (2007).

107 **Insert figure 2**

108 *2.2. Thick-skinned tectonic*

109 Some authors, using seismological data from Taiwan front orogen (Wu et
110 al., 1997) or well-log and seismic reflection data (Hung et al., 1999) disagree
111 with the thin-skinned tectonic. They propose that the detachment is actually
112 in the basement. In this case, the deformation would be accommodated by

113 the re-activation of normal faults created by the Paleogene rifting opening
114 the Chinese Sea (Mouthereau & Petit, 2003), into reverse faults. According
115 to Wu et al. (1997), the Taiwanese orogeny involves the whole crust and the
116 upper mantle, in particular beneath the Central Range. They suggest litho-
117 spheric collision between the Eurasian and the Philippine Sea plates.

118 Mouthereau & Petit (2003) explain that, to accommodate this thick-skinned
119 deformation, the detachment must belong to a weak part of the crust, prob-
120 ably at the brittle/ductile discontinuity. The dense fractures concentration
121 in the upper crust compared to the lower crust and the lithospheric mantle
122 make the latter appears less elastic and strong. The decoupling would then
123 exists between the upper crust and the lower crust/mantle group. These
124 indications are used to draw the thick-skinned structure (figure 3).

125 **Insert figure 3**

126 **3. Deformation modeling**

127 *3.1. Elastic deformation modeling*

128 Our elastic deformation code uses dislocation equations from Okada (1985,
129 1992) to compute the ground movements, vertically and horizontally, gener-
130 ated by faults slipping in an elastic half-space. The faults are defined by
131 their geometry and their movement. After running, we compare the mod-
132 eled horizontal movements with those measured by GPS. We proceed by trial
133 and error to find the best adjustment between model and data. Attention is
134 given to actual geophysics and geologic data already available from Taiwan
135 structure to ensure the likelihood of our model.

136 We used the horizontal GPS velocities published by Hickman et al. (2002)

137 based on measurements performed in 1996 and 1997. GPS velocities are
138 computed relative to the SR01 station on Penghu Islands, i.e. in a Eurasia
139 fixed reference frame. Due to the small interval between the measurements,
140 vertical velocities are not usable to constrain the elastic models. Only GPS
141 stations within a band of 10 km wide on both side of the studied transect
142 are taken into account. Modeling will be performed using thick-skinned and
143 thin-skinned models, for which geometries are different. However some basic
144 modeling ideas are the same in both cases:

- 145 1. Faults are mapped following the geological map of Taiwan. We also
146 add a large detachment beneath Taiwan. All the faults have a reverse
147 movement.
- 148 2. The slip rate on the eastern part of the detachment is set to 82 mm yr^{-1} ,
149 corresponding to the Philippine Sea plate - Eurasian plate convergence
150 rate (Yu et al., 1997).
- 151 3. The slip rate of the detachment decreases from East to West.
- 152 4. The faults start from the surface and stop on the detachment. They
153 are divided into two segments to better represent their actual geometry,
154 which dip is not constant (Hsu et al., 2003) and to allow depth-variable
155 slip rates.
- 156 5. All the fault slip in depth and are locked close to the surface (Lo-
157 evencruck et al., 2001) except the Longitudinal Valley fault where
158 30 mm yr^{-1} creep exists up to the surface (Lee et al., 2006).
- 159 6. Apart the Longitudinal Valley, the shortening of Taiwan is mostly ac-
160 commodated within the Western Foothills faults (Simoes & Avouac,
161 2006). We consequently assume higher slip rate in this region.

162 *3.2. Thick skinned tectonic results*

163 The best-fit model is shown on figure 4. The detachment starts from the
164 West at 15 km depth and slightly dips (3°) to the East (figure 4 a). This
165 model underestimates the westward velocities in the Western Foothills and
166 the Coastal Range, respectively 20 % and 17 % lower (figure 4 b). These
167 too low velocities are due to the highly dipping faults, which cannot generate
168 strong horizontal movements but return high vertical movements (figure 4 c).
169 Moreover, due to the depth of the detachment, the faults slip at great depth,
170 reducing the movement created on the ground.

171 **Insert figure 4**

172 The thick-skinned model returns vertical movements from 0 to 2.6 cm yr^{-1} ,
173 i.e. only surrection. The greatest elevation rates are in the Western Foothills
174 and in the Coastal Range, where there are reverse faults. It illustrates the up-
175 ward movement of their hanging wall. The Longitudinal Valley fault returns
176 the higher elevation rate, 2.6 cm yr^{-1} , in the Coastal Range.

177 *3.3. Thin-skinned tectonic results*

178 Here the detachment starts at 5 km depth, beneath the Coastal Plain
179 and slopes down to 10 km depth beneath the Coastal Range, with 3° dip
180 (figure 5 a). This model fits well the horizontal GPS velocities (figure 5 b).
181 This agrees with Hsu et al. (2003) who have shown that a thin-skinned model
182 is able to fit the horizontal GPS velocities.

183 **Insert figure 5**

184 Vertical movements (figure 5 c) remain higher in the Western Foothills and
185 the Coastal Plain, but are not as great and wide as with the thick-skinned
186 model. We predict 1.5 cm yr^{-1} of maximum elevation versus 2.6 cm yr^{-1}

187 with the thick-skinned tectonic. Thin-skinned tectonic involves faults with
188 a lower dip, which slip creates high horizontal movements but small vertical
189 movements. This is well illustrated by comparing movements generated by
190 the Longitudinal Valley, Tingpinglin or Lunhou faults for each model (fig-
191 ures 4 and 5). Consequently westward movements are not underestimated
192 anymore and the modeled elevation rate decreases in the Western Foothills.
193 The other parameter improving the adjustment of the model to the hori-
194 zontal GPS velocities is the lower depth of the detachment, its slip is less
195 attenuated on the ground since it is closer to the surface than it was with
196 the thick-skinned tectonic. No particular surrection of the Central Range is
197 predicted, even with the thick-skinned model. This is characteristic of any
198 model in which most of the convergence is transferred across Taiwan to the
199 Western Foothills (Hsu et al., 2003).

200 **4. Gravity modeling**

201 We use Granom (Hetényi et al., 2007), a code computing gravity anomaly
202 based on Won & Bevis (1987) algorithm, to calculate the gravity changes
203 involved by the deformation modeled in paragraph 3. Applying densities
204 on the 2D structure, we calculate the gravity anomaly generated before and
205 after the elastic deformation. Subtracting these anomalies from each other,
206 the gravity change owing to deformation is obtained.

207 *4.1. Density model*

208 In addition to an increase of the density value with depth, the strong
209 lateral heterogeneity of materials in Taiwan is also taken into account. Sed-
210 iments in the Coastal Plain are little condensed while the orogen, which

211 extends from the Western Foothills to the Coastal Range, experiences ex-
212 humation of deep, i.e. high density, rocks (Dahlen et al., 1984). The Coastal
213 Range, as part of the oceanic crust, is denser than continental crust materi-
214 als. According to Dahlen et al. (1984) and Lin & Watts (2002), the following
215 scheme is applied:

- 216 1. Sedimentary basin (Coastal Plain): 2.5 (2500 kg m^{-3})
- 217 2. Topographic load (Western Foothills, Slate Belt and Central Range)
218 and middle crust: 2.7 (2700 kg m^{-3})
- 219 3. Oceanic crust (Coastal Range and eastern regions) and lower crust: 2.8
220 (2800 kg m^{-3})

221 Areas of different densities are bounded with the faults and depth threshold
222 used in each model. Hence the regions with same density will have different
223 size depending on the tectonic model, thick or thin-skinned.

224 4.2. Modeling

225 Whatever the tectonic, comparing the elevation rate modeled (figure 6 a
226 and b) with gravity changes (figure 6 c) underlines the free-air effect, the
227 gravity decreases when altitude increases. The shape of gravity changes is
228 indeed the opposite to vertical movements. Using the mean free-air gradient
229 -0.3086 mGal for one meter elevation, we remove this effect and obtain the
230 figure 6 d.

231 **Insert figure 6**

232 The plate effect is here well illustrated as gravity changes have the same trend
233 as vertical elevation. This can be demonstrated plotting gravity changes
234 versus elevation rate, which gives a slop of $0.1138 \text{ mGal m}^{-1}$ with a good

235 determination coefficient. If we now estimate the plate effect using the mean
236 $0.0419 \rho \text{ mGal m}^{-1}$ and a mean density 2.67, we obtain $0.1118 \text{ mGal m}^{-1}$,
237 which is very close to the slope given in regression equation. Gravity changes
238 are then dominated by free-air and plate effect, involving several μGal of
239 change each year.

240 Also removing plate effect we obtain gravity changes only due to mass trans-
241 fers (figure 7). They are low, around ten times smaller than free-air and
242 plate effects. The thick-skinned tectonic returns higher gravity changes, up
243 to $0.3 \mu\text{Gal yr}^{-1}$ while the thin-skinned tectonic profile is almost constant,
244 near zero. The step at distances 0 and 80 km, for both tectonics, may be
245 explained by the lateral change of density at the surface, respectively from
246 2500 to 2700 kg m^{-3} and 2700 to 2800 kg m^{-3} and do not give indications
247 on deep mass transfers. The thick-skinned signal in the east part of Taiwan
248 may be interpreted as the overhang of the Coastal Range and oceanic crust
249 dense rocks on the continental crust beneath the Central Range. The gravity
250 decrease, which extends from the Western Foothills to the Central Range, is
251 more complicated to explain. One hypothesis could be the slip on the de-
252 tachment and the global westward propagation of the whole system, which
253 slightly replaces lower crust with upper material, less dense.

254 **Insert figure 7**

255 With more confidence we can suggest that the thick-skinned tectonic gener-
256 ates higher gravity changes since, with its geometry, it involves higher rock
257 volumes, hence higher mass transfers.

258 5. Discussion

259 We obtain the best fit between the modeled horizontal velocities and
260 those estimated by GPS using the thin-skinned tectonic geometry. The
261 thick-skinned tectonic can model the global trend of the westward horizontal
262 movements, i.e. a growing amplitude from West to East, but quantitatively
263 values are underestimated of $\sim 20\%$. Yet we do not reject this tectonic
264 hypothesis since the horizontal GPS velocities we used contain uncertainties
265 involved by the short delay between campaigns (see paragraph 3.1). Hence,
266 they cannot be considered as absolute discriminant factors. In addition we
267 use elastic modeling, which may show limitations when applied for complex
268 rheology. The fact that we do not represent the subduction of the Eurasian
269 plate beneath the Philippine Sea plate betrays this limitation: it exists in
270 the region we study, consequently the detachment we draw beneath Taiwan
271 should slop down eastward with an increasing dip. But this geometry fails
272 to make modeled horizontal velocities fit GPS data.

273 Concerning vertical movements, Chen (1984) found that the Central Range
274 rises faster than the Coastal Range but we do not retrieve this observation.
275 West of the Longitudinal Valley the modeled shortening is accommodated by
276 faults of the Western Foothills, which consequently rises. Our elastic model
277 cannot generate surrection in the Central range since there is no active fault
278 in this region. Simoes & Avouac (2006) suggest that the Central Range
279 surrection can be explained by underplating of the upper seven km of the
280 Eurasian crust beneath the orogen, during the convergence of the Philippine
281 Sea plate toward the Chinese continental margin. The shortening accommo-
282 dation occurs in the Western Foothills where an accretionary prism grows,

283 but there is no accretion in the intern part of the orogen ; its rising and ex-
284 humation are consequences of this underplating. It is typically a deep mass
285 transfer and must be taken into account for accurate gravity modeling. Be-
286 havior finer than pure elasticity, allowing thermokinematic deformation, is
287 likely to simulate this phenomenon.

288 The vertical movements of the Central Range lead to two major issues. The
289 first one is the uncertainty attributed to GPS data; determining vertical ve-
290 locities using GPS requires at last one decade to obtain robust results. The
291 second one is to use the appropriate deformation model to fit the vertical
292 velocities. Both issues involve uncertainty of the estimation of the gravity
293 signal due to vertical movement, i.e. free-air and plate effect, which represent
294 the most important part of the total gravity signal expected from mountain
295 building. The mass transfer gravity signal, far smaller in comparison, has
296 consequently a large uncertainty.

297 One must note that we do not model any hydrological effect. Yet it can
298 reaches values above $10 \mu\text{Gal}$ due to local variations of groundwater height
299 (Naujoks et al., 2008; Jacob et al., 2008). This amplitude may hide or deprave
300 the expected tectonic effects; some μGal per year according to our modeling.
301 Actually, AG sites have been also selected to minimize hydrological influence.
302 From AG1 to AG6, pillars are located in mountains and directly built on the
303 rock basement. Water is supposed to bypass in these areas without being
304 stored inside the thin soil cover. Nevertheless, this situation is not possible
305 for AG7 and AG8, which are in the Coastal Plain, i.e. a sedimentary basin
306 covering the west side of Taiwan and containing several aquifers. We must
307 hence pay special attention to groundwater height for these two sites, using

308 aquifer monitoring performed in Taiwan. Moreover aquifers in this region
309 suffer from over-pumping involving subsidence rates higher than 1 cm yr^{-1}
310 (Hou et al., 2005; Hu et al., 2006). This movement is likely to have effect on
311 gravity value but must absolutely be identified since we just consider tectonic
312 phenomena.

313 Modern absolute gravimeters have a sensitivity around $1 \mu\text{Gal}$, yet the grav-
314 ity changes we model, only concerning mass transfers, reaches maximum
315 $0.3 \mu\text{Gal yr}^{-1}$. At least three years are hence needed between two mea-
316 surements to see deep mass transfer effects. But only one year should offers
317 interesting results since we predict up to $5 \mu\text{Gal yr}^{-1}$ due to elevation. AGTO
318 should consequently sort out the tectonic component of gravity in Taiwan.

319 6. Conclusion

320 The aim of this paper was to give preliminary ideas of what signal can
321 be expected from the AGTO project, using elastic deformation and gravity
322 modeling for two main tectonic contexts: thick-skinned and thin-skinned.
323 Our results show higher elevation rates in the Western Foothills and the
324 Coastal Range reaching respectively 1.5 and 2 cm yr^{-1} for the thin-skinned
325 tectonic and 2.2 and 2.6 cm yr^{-1} for the thick-skinned. The gravity changes
326 are maximum in the same regions; respectively 3.8 and $4 \mu\text{Gal yr}^{-1}$ for
327 the thin-skinned tectonic and 4.5 and $5 \mu\text{Gal yr}^{-1}$ for the thick-skinned.
328 Yet most of this signal is free-air and plate effects, mass transfers effects
329 are ten times lower: $0.1 \mu\text{Gal yr}^{-1}$ assuming a thin-skinned tectonic and
330 $0.3 \mu\text{Gal yr}^{-1}$ with the thick skinned. Both are expected in the Coastal
331 Range where density contrast and movement along the Longitudinal Valley,

332 the plate boundary between Eurasian and the Philippine Sea plates, are
333 significant. As this yearly signal is very low, it will be difficult to identify
334 without robust GPS and hydrological constraints and long time series. Our
335 modeling fails to reproduce the Central Range surrection, which is known to
336 be the fastest elevated region of Taiwan (Chen, 1984; Hsu et al., 2003; Wu
337 et al., 1997). Such a misfit can be related to the elastic behavior we assume
338 in our modeling, while a more complicated rheology may be involved. This
339 surrection is supposed to be driven by underplating below the orogen (Simoes
340 & Avouac, 2006), that we do not model in our study. The absolute gravity
341 measurements will first reflect the vertical movements in Taiwan and then
342 deep mass transfers for which several years of measurement should be needed
343 before any interpretation. GPS measurements will have a strong interest to
344 precisely separate elevation and deep mass transfer effects.

345 **7. Acknowledgments**

346 We are grateful to John B. Hickman for providing us with GPS velocities
347 data. We also thank György Hetényi for his guidance in our use of Granom
348 program. Figure 1 has been drawn with Generic Mapping Tools - GMT
349 (Wessel & Smith, 1998).

350 **References**

- 351 Angelier, J., 1986. Preface. *Tectonophysics* 125.
- 352 Chapple, W. M., 1978. Mechanics of thin-skinned fold-and-thrust belts. *Geol.*
353 *Soc. Am. Bull.* 89, 1189-1198.

- 354 Chen, H., 1984. Crustal uplift and subsidence in Taiwan: an account based
355 upon retriangulation results. *Spec. Publ. Cent. Geol. Surv.* 3, 127-140.
- 356 Dahlen, F. A., Suppe, J., Davis, D., 1984. Mechanics of fold-and-thrust belts
357 and accretionary wedges: cohesive Coulomb theory. *J. Geophys. Res.* 89
358 (B12), 10,087-10,101.
- 359 Davis, D., Suppe, J., Dahlen, F.A., 1983. Mechanics of fold-and-thrust belts
360 and accretionary wedges. *J. Geophys. Res.* 88 (B2), 1153-1172.
- 361 Hetényi, G., Cattin, R., Brunet, F., Bollinger, L., Vergne, J., Nábělek, J.
362 L., Diament, M., 2007. Density distribution of the India plate beneath the
363 Tibetan Plateau: geophysical and petrological constraints on the kinetics
364 of lower-crustal eclogitization. *Earth Planet. Sci. Lett.* 264 (1-2), 226-244,
365 doi: 10.1016/j.epsl.2007.09.036
- 366 Hickman, J. B., Wiltschko, D. V., Hung, J.-H., Fang, P., Bock, Y., 2002.
367 Structure and evolution of the active fold-and-thrust belt of southwestern
368 Taiwan from Global Positioning System analysis. In: Byrne, T.B., and Liu,
369 C.-S. (Ed.), *Geology and geophysics of an arc-continent collision, Taiwan:*
370 *Boulder, Colorado, Geological Society of America Special Paper, # 358,*
371 *pp. 75-92.*
- 372 Ho, C. S., 1986. A synthesis of the geologic evolution of Taiwan. *Tectono-*
373 *physics* 125, 1-16.
- 374 Hou, C.-S., Hu, J.-C., Shen, L.-C., Wang, J.-S., Chen, C.-L., Lai, T.-C.,
375 Huang, C., Yang, Y.-R., Chen, R.-F., Chen, Y.-G., Angelier, J., 2005.

- 376 Estimation of subsidence using GPS measurements, and related hazard:
377 the Pingtung Plain, southwestern Taiwan. *C.R. Geosci.* 337, 1184-1193.
- 378 Hsu, Y.-J., Simons, M., Yu, S.-B., Kuo, L.-C., Chen, H.-Y., 2003. A two-
379 dimensional dislocation model for interseismic deformation of the Taiwan
380 mountain belt. *Earth Planet. Sci. Let.* 211, 287-294.
- 381 Hu, J.-C., Chu, H.-T., Hou, C.-S., Lai, T.-H., Chen, R.-F., Nien, P.-F., 2006.
382 The contributor to tectonic subsidence by groundwater abstraction in the
383 Pingtung area, southwestern Taiwan as determined by GPS measurements.
384 *Quat. Int.* 147, 62-69.
- 385 Hung, J.-H., Wiltschko, D. V., Lin, H.-C., Hickman, J. B., Fang, P., Bock,
386 Y., 1999. Structure and motion of the southwestern Taiwan fold-and-thrust
387 belt. *TAO* 10 (3), 543-568.
- 388 Jacob, T., Bayer, R., Chéry, J., Jourde, H., Le Moigne, N., Boy, J.-P., Hin-
389 derer, J., Luck, B., Brunet, P., 2008. Absolute gravity monitoring of water
390 storage variation in a karst aquifer on the larzac plateau (Southern France).
391 *Journal of Hydrology* 359, 105-117.
- 392 Karner, G.D., Watts, A.B., 1983. Gravity anomalies and flexure of the litho-
393 sphere at mountain ranges. *J. Geophys. Res.* 88 (B12), 10,449-10,477.
- 394 Kim, K.-H., Chiu, J.-M., Pujol, J., Chen, K.-C., Huang, B.-S., Yeh, Y.-H.,
395 Shen, P., 2005. Three-dimensional VP and VS structural models associated
396 with the active subduction and collision tectonics in the Taiwan region.
397 *Geophys. J. Int.* 162, 204-220.

- 398 Lee, J.-C., Chu, H.-T., Angelier, J., Hu, J.-C., Chen, H.-Y., Yu, S.-B., 2006.
399 Quantitative analysis of surface coseismic faulting and postseismic creep
400 accompanying the 2003, Mw = 6.5, Chengkung earthquake in eastern Tai-
401 wan. *J. Geophys. Res.* 111, B02405, doi:10.1029/2005JB003612.
- 402 Lin, A. T., Watts, A. B., 2002. Origin of the west Tainan basin by orogenic
403 loading flexure of a rifted continental margin. *J. Geophys. Res.* 107 (B9),
404 2185, doi: 10.1029/2001JB000669.
- 405 Loevencruck, A., Cattin, R., Le Pichon, X., Courty, M.-L., Yu, S.-B., 2001.
406 Seismic cycle in Taiwan derived from GPS measurements. *C. R. Acad. Sci.*
407 Paris, *Earth. Planet. Sci. Let.* 333, 57-64.
- 408 Malavieille, J., Trullenque, G., In press, Corrected proof. Consequences of
409 continental subduction on forearc basin and accretionary wedge deforma-
410 tion in SE Taiwan: insights from analogue modeling. *Tectonophysics*.
- 411 Mouthereau, F., Petit, C., 2003. Rheology and strength of the Eurasian con-
412 tinental lithosphere in the foreland of the Taiwan collision belt: constraints
413 from seismicity, flexure, and structural styles. *J. Geophys. Res.* 108 (B11),
414 2512, doi: 10.1029/2002JB002098.
- 415 Naujoks, M., Weise, A., Kroner, C., Jahr, T., 2008. Detection of small hydro-
416 logical variations in gravity by repeated observations with relative gravime-
417 ters. *J. Geod.* 82, 543-553, doi:10.1007/s00190-007-0202-9.
- 418 Okada, Y., 1985. Surface deformation due to shear and tensile faults in a
419 half-space. *Bull. Seism. Soc. Am.* 75, 1135-1154.

- 420 Okada, Y., 1992. Internal deformation due to shear and tensile faults in a
421 half-space. *Bull. Seism. Soc. Am.* 82, 1018-1040.
- 422 Shin, T.-C., Teng, T.-L., 2001. An overview of the 1999 Chi-Chi, Taiwan
423 earthquake. In Dedicated issue on the Chi-Chi, Taiwan earthquake of 20
424 September 1999, *Bull. Seism. Soc. Am.* 91,895-913
- 425 Simoes, M., Avouac, J. P., 2006. Investigating the kinematics of the moun-
426 tain building in Taiwan from the spatiotemporal evolution of the fore-
427 land basin and western foothills. *J. Geophys. Res.* 111, B10401, doi:
428 10.1029/2005JB004209.
- 429 Segall, P., Davis, J.L., 1997. GPS applications for geodynamics and earth-
430 quake studies. *Annu. Rev. Earth Planet. Sci.* 25, 301-336.
- 431 Suppe, J., 1980. A retrodeformable cross section of northern Taiwan. *Geol.*
432 *Soc. China Proc.* 23, 46-55.
- 433 Torge, W., 1990. Absolute gravimetry as an operational tool for geodynamics
434 research. In: Springer Berlin / Heidelberg (Ed.), *Developments in Four-*
435 *Dimensional Geodesy, Book Series Lecture Notes in Earth Sciences*, 29,
436 pp. 15-28.
- 437 Wessel, P., Smith, W. H. F., 1998. New, improved version of Generic Mapping
438 Tools released. *EOS Trans. Amer. Geophys. U.* 79 (47), pp. 579.
- 439 Won, I. J., Bevis, M., 1987. Computing the gravitational and magnetic
440 anomalies due to a polygon: Algorithms and Fortran subroutines. *Geo-*
441 *physics* 52, 232-238.

- 442 Wu, F.-T., Rau, R.-J., Salzberg, D., 1997. Taiwan orogeny: thin-skinned or
 443 lithospheric collision? *Tectonophysics* 274, 191-220.
- 444 Yu, S.-B, Chen, H.-Y., Kuo, L.-C., 1997. Velocity field of GPS stations in
 445 the Taiwan area. *Tectonophysics* 274, 41-59.

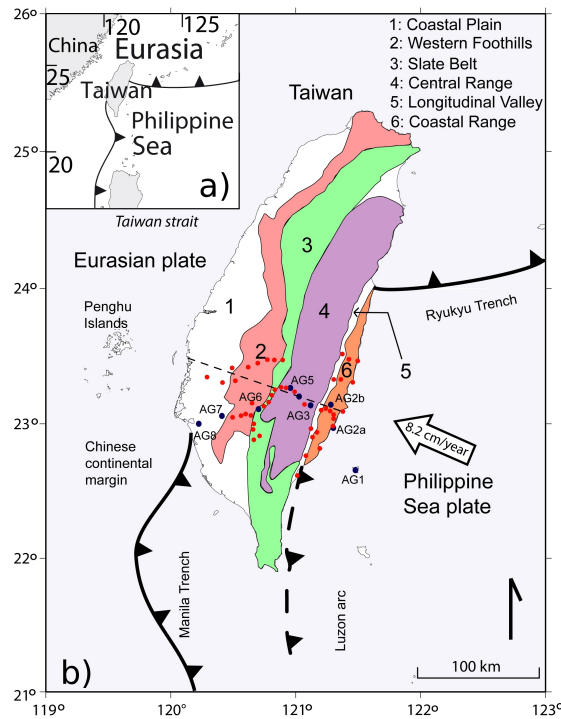


Figure 1: (a) Global location and plate tectonic settings, (b) General geology of Taiwan after Ho (1986) and Hickman et al. (2002). The nine sites for absolute gravity measurements of the AGTO project, from AG1 to AG8, are represented (blue dots) with also the 45 sites defined for relative gravity measurements network (red dots). Our 2D modeling study is performed along the dashed line.

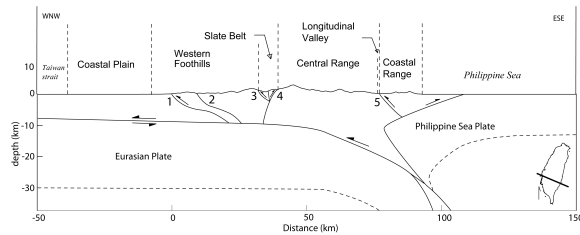


Figure 2: Thin-skinned tectonic structure (after Malavieille & Trullenque (2007)). The detachment starts West at 10 km depth, between the basement and the sediment cover, and slopes down eastward below the Central Range. Faults join the detachment but do not cross it. Numbers refer to faults: 1-Lunhou, 2-Tingpinglin, 3-Tulungwan, 4-Lishan, 5-Longitudinal Valley fault.

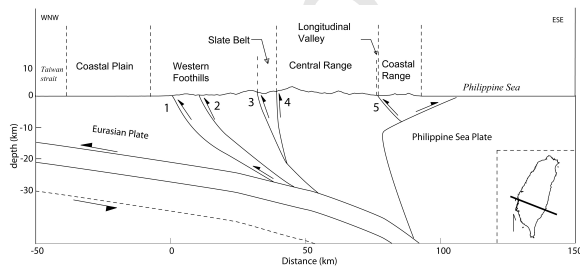


Figure 3: Thick-skinned tectonic structure (After Mouthereau & Petit (2003) for the part West of the Central range). The detachment is deeper than in the thin-skinned structure, between the upper crust and the mantle. Also see figure 2 for faults numbers meaning.

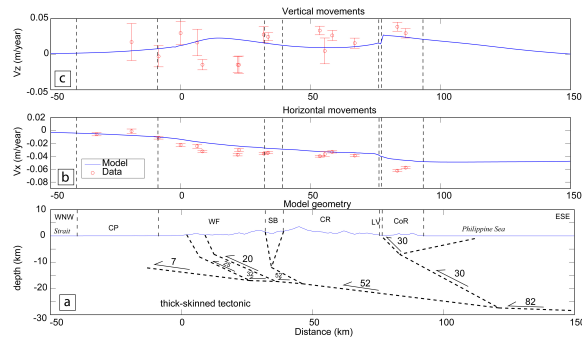


Figure 4: From bottom to top: (a) Model geometry and cinematic, faults are dashed lines, arrows indicates movements directions, values are slip velocities in mm yr^{-1} . Abbreviations: CP=Coastal Plain ; WF=Western Foothills ; SB=Slate Belt ; CR=Central Range ; LV=Longitudinal Valley ; CoR=Coastal Range. (b) Horizontal movements measured (red circles) and modeled (plain blue line), positive values mean eastward movement. (c) Vertical movements measured (red circles) and modeled (plain blue line), positive values mean upward movement. We adjust modeled horizontal movements to estimated ones.

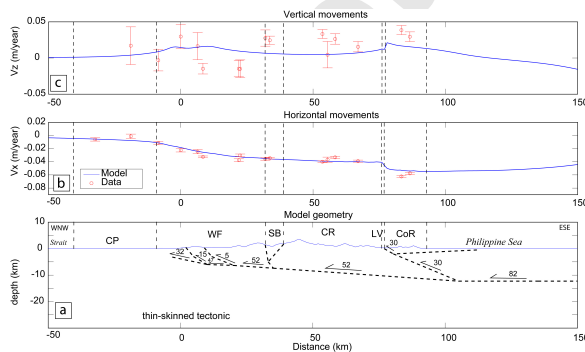


Figure 5: Same as figure 4 but considering a thin-skinned tectonic. This geometry allows a better adjustment of modeled horizontal movements to estimated ones, in particular in the Western Foothills and the Longitudinal Valley. Also see figure 4 for abbreviations.

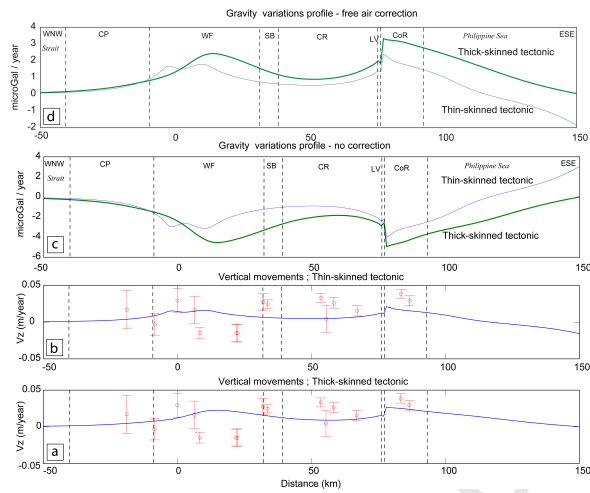


Figure 6: Graphs (a) and (b) are respectively the modeled vertical movements for thick-skinned tectonic and thin-skinned tectonic (already shown in figures 4 c and 5 c). (c) Gravity changes modeled with thin (fine blue line) and thick-skinned (bold green line) tectonic. Note the symmetry between vertical movements and the gravity signal, which reflects free-air effect. (d) Same as (c) but the gravity signal has been corrected from free-air effect. Its shape has now the same trend as vertical movements, for each tectonic. The plate effect is here responsible for the main part of the gravity signal. Also see figure 4 for abbreviations.

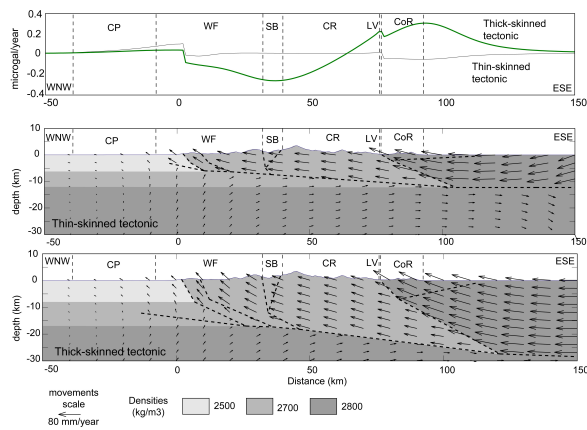


Figure 7: Gravity changes modeled for the two hypothesis, thin-skinned (fine blue line) and thick skinned tectonic (bold green line), and only due to mass transfers. Free-air and plate effects have been removed. The thick-skinned tectonic returns the higher gravity changes in the Coastal range with $0.3 \mu\text{Gal yr}^{-1}$, while the thin-skinned tectonic reaches maximum $0.1 \mu\text{Gal yr}^{-1}$. The greyscale gives the density model and the arrows indicate the structure movements. Also see figure 4 for abbreviations.